DOI: 10.26599/FSHW.2026.9251017

Contents lists available at SciOpen

Food Science and Human Wellness

journal homepage: https://www.sciopen.com/journal/2097-0765

China Food Publishing Co.

Deciphering Ecological Interactions in Oral Microbiome Remodelling Associated with Aging-Induced Taste Sensitivity Decline: a case study in Fangshan District, Beijing, China

Sizhe Qiu[1,2‡], Haojie Ni[1‡], Aidong Yang[2], Hong Zeng[1*], Yanbo Wang[1*]

[1]*School of Food and Health, Beijing Technology and Business University, 100048, China*

[2]*Department of Engineering Science, University of Oxford, OX1 3PJ, United Kingdom*

ABSTRACT: Aging-induced taste sensitivity decline, recognized as a world-wide health issue, has shown considerable modulatory effects on the oral microbiome that serves as an etiological driver for multiple dysbiosis-associated diseases. However, the underlying ecological interactions remain poorly characterized. Therefore, this study conducted oral metagenomic/metabolomic analysis for youth/elderly individuals with different taste sensitivities. Results showed that elevated fatty acid levels in elderly samples with low taste sensitivity drove a metabolic adaptation of the oral microbiome that the substrate preference of energy metabolism altered from monosaccharides to fatty acids, which resulted in the remodelling of the oral microbiome composition. In addition, the up-regulation of *Prevotella* species engaging in active quorum sensing interactions with other oral bacteria in elderly samples was found to affect oral microbiome remodelling. Furthermore, community-level metabolic modeling and synthetic co-culture experiments revealed and validated that interspecies nutrient feeding contributed to the oral microbiome remodelling. Collectively, these findings elucidated the modulatory effects of aging-induced taste sensitivity decline on the oral microbiome by decoding the ecological Interactions of key oral bacteria and metabolites, paving the way for developing viable strategies for oral microbiome rehabilitation.

Keywords: Taste sensitivity; Aging; Oral microbiome; Multi-omics; Quorum sensing; Metabolic interactions;

1. Introduction

With the rapid acceleration of global population aging, aging-induced health issues, especially deterioration of sensory functions that substantially compromises life quality, have gained great attention [1]. As a representative aging-induced health issue, taste sensitivity decline has been considered as an influential problem across different countries, which largely lowers the food hedonics and overall well-being of elderly population [2]. It has been well recognized that taste sensitivity decline can change the dietary habits of elderly people by leading them to choose strong-flavor foods, especially high-fat/sugar foods [3]. One direct impact of such unhealthy dietary habits is the imbalance of the oral microbiome, also known as oral dysbiosis [4], which can lead to obesity, diabetes, and many other metabolic issues [5–7]. Meanwhile, oral bacteria has also been

‡Equal contribution
***Corresponding author**
zenghong@btbu.edu.cn (H. Zeng); wyb1225@163.com (Y. Wang)

Received 31 December 2025
Received in revised from 29 January 2026
Accepted 12 February 2026

found to affect taste sensitivity by altering the concentrations of tastants [8,9]. Briefly, there is a noteworthy interplay between taste sensitivity changes and the oral microbiome that warrants further study.

To investigate the entangled relationship between taste sensitivity and oral microbiome, studies in recent years have conducted taste sensitivity evaluation and metagenomic analysis to identify key bacteria associated with taste thresholds [10]. For instance, Cattaneo et al., 2019 discovered that *Actinomyces*, *Oribacterium*, *Solobacterium*, *Catonella*, and *Campylobacter* had significantly higher abundance levels in oral samples of high taste sensitivity [8]; Licandro et al., 2023 found 109 bacterial species correlated with the sensitivity of at least one taste in sweetness, sourness, bitterness, saltiness, and umami, and some species (e.g., *Streptococcus parasanguinis*) correlated with multiple taste sensitivities [11]. However, those correlational studies are inherently unable to unravel the functional roles of key oral bacteria and metabolites or to establish in-depth mechanisms to explain the modulation of oral microbiomes associated with aging-induced taste sensitivity decline.

Aiming to address the above knowledge gap and gain a mechanistic understanding of how aging-induced taste sensitivity decline remodels the oral microbiome, this study adopted a multi-omics fusion analysis workflow that integrated oral metagenomics and metabolomics of youth and elderly individuals in Fangshan district, Beijing, China. This study hypothesized that oral metagenomics and metabolomics could elucidate the ecological interactions of key oral bacteria and metabolites that lead to the oral microbiome remodelling associated with aging-induced taste sensitivity decline. Apart from conventional differential abundance and correlation analysis of oral bacteria and metabolites, this study analyzed functional pathway abundance and quorum sensing (QS) activities of the oral microbiome, and constructed community-level metabolic models to simulate interspecies metabolic interactions. Moreover, mono- and co-culture experiments were conducted to validate observed and model-inferred ecological interactions of oral bacteria and metabolites. Overall, this study attempted to decipher the functional roles and ecological interactions of key oral bacteria and metabolites, and reveal how aging-induced taste sensitivity decline remodels the oral microbiome.

2. Materials and Methods

2.1 Taste sensitivity test across two age groups

20 individuals were recruited for taste sensitivity test in Aug-Sept 2024 and separated into two groups based on ages: A group (n=10) for 20~30 years old and B group (n=10) for 55~80 years old (**Figure 1**). Individuals of A group were recruited from Beijing Technology and Business University (Fangshan, Beijing, China), and individuals of B group were recruited from communities in Fangshan District, Beijing, China. Detailed information of all 20 participants was presented in Table S1 in Supplementary Materials. The exclusion criteria were: smokers, pregnancy or lactation, using antibiotics or undergoing specific dental treatments within the past three months. All 20 participants reported no oral or metabolic diseases and no medication use. Each participant was asked not to eat or drink (allow water) for one hour before the experiment. This study was conducted according to the Declaration of Helsinki and approved by the Scientific

Research Ethics Committee of Beijing Technology and Business University (No. 2024-118 and No. 2024-119, approved on 15/04/2024). Informed consent was obtained from all participants.

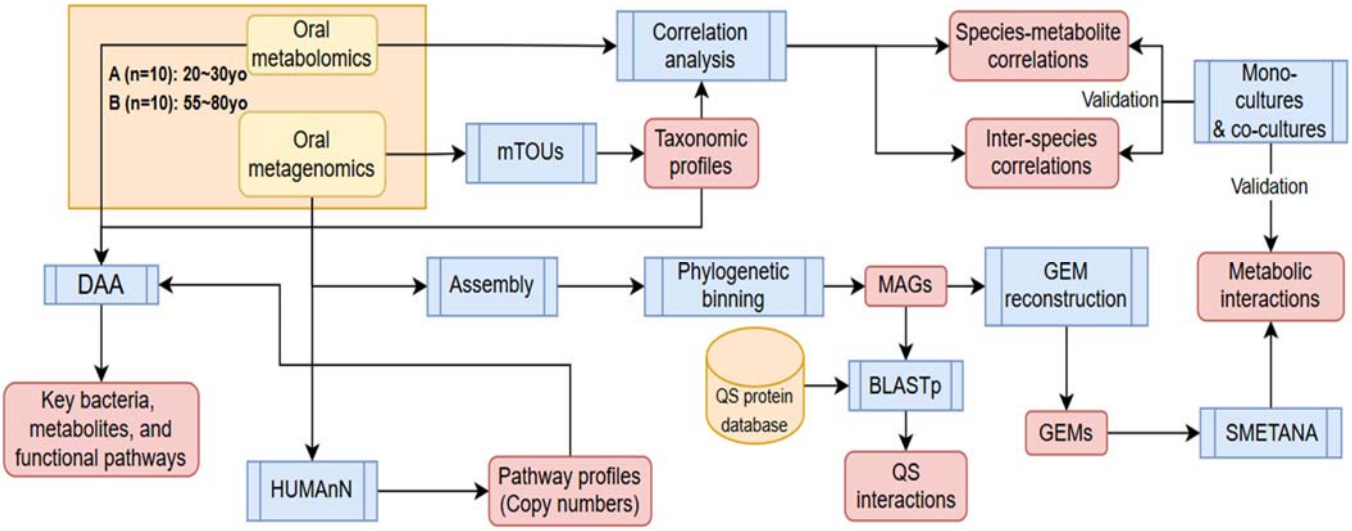


Figure 1. Multi-omics fusion analysis workflow of oral metagenomics and metabolomics. DAA: differential abundance analysis; MAG: metagenome assembled genome; QS: quorum sensing; GEM: genome-scale metabolic model; SMETANA: species metabolic interaction analysis.

Sweetness was selected for the taste sensitivity test, as the decline in sweet taste sensitivity has been identified as one of the most significant taste perception deteriorations in elderly population [12] and the response to sweetness has been widely recognized to influence food hedonics, food choices, dietary acceptability and overall well-being [13,14]. The sensitivity threshold test, according to ascending three-alternative forced choice [15], was conducted to quantify sweet taste sensitivity of individuals of A and B groups. A series of sucrose solutions with varying concentrations, prepared using pure water, served as sweet stimuli. Sucrose concentration levels were determined based on the standards of ISO 3972 with minor modifications [16] . The first sample was pure water, followed by sucrose solutions in ascending order of concentration: from 2.59 g/L to 33.33 g/L for the B group with a geometric ratio of 0.6, and from 0.34 g/L to 12 g/L for the A group (R=0.6) with the addition of 0.14 g/L and 0.24 g/L concentrations. This concentration range was designed to cover inter-individual differences in taste sensitivity, as well as to allow for sorting expected individuals with heightened thresholds in the B group of old ages and lower thresholds in the A group of young ages. A sample evaluation procedure was performed similarly to the reported work [17]. The detection threshold (DT) and the recognition threshold (RT) were calculated as $DT/RT = \sqrt{C_n \times C_{n+1}}$, C_n was the last not correctly identified concentration and C_{n+1} was the next higher correctly identified concentration.

2.2 Metagenomic sequencing and analysis of the oral microbiome

Unstimulated saliva was collected with 5 mL sterile plastic tubes (Suqian Wuwang Trading Co., LTD, Jiangsu, China), and stored at -80 ºC. Genomic DNA was extracted by FastPure Stool DNA Isolation Kit (Magnetic bead) (MJYH, Shanghai, China). After quality assessment with SynergyHTX and NanoDrop2000, the DNA extract was fragmented to an average size of about 350 bp using Covaris M220 (Gene Company Limited, China) for paired-end library construction. The paired-end library was constructed using

NEXTFLEX Rapid DNA-Seq (Bioo Scientific, Austin, TX, USA). Paired-end sequencing was performed on Illumina NovaSeq X Plus (Illumina Inc., San Diego, CA, USA) with PE150 reads length.

The raw reads of metagenomic sequencing were cleaned to remove human reads and keep only high-quality reads with quality values higher than 38 and length longer than 350 bp. After the quality control step, the cleaned reads were assembled by MEGAHIT [18] with default parameters. The species-level taxonomic profile was computed using mOTUs profiler [19]. With the mOTUs database version 3.1.0, the profiler identified species and computed relative genomic abundance levels with unassembled DNA reads.

MetaBAT2 [20], MaxBin2 [21] and CONCOCT [22] were used for phylogenetic binning. Binned metagenome assembled genomes (MAGs) from three different tools were refined with the completeness and contamination cutoffs of 90% and 10% using the refinement module in metaWRAP [23]. GTDB-Tk [24] was used to classify the taxonomy of each refined MAG. Those MAGs' genomic abundances in each sample were computed by Salmon [25], which aligned and counted reads from each sample to estimate the abundance of each contig.

Protein-coding genes were predicted for assembled genomes and binned MAGs by Prodigal [26]. Functional analysis of the metagenome was conducted using HUMAnN-3.0 [27]. To annotate quorum sensing (QS) proteins in MAGs, BLASTp [28] was used to compare 213 recognized QS proteins from SigMol and Quorumpeps databases [29–31] with protein sequences of high-quality MAGs obtained in this study. For parameters of BLASTp, the expectation value (e-value) was 1e-6 and the maximum target number was set as 5.

2.3 Reconstruction of genome-scale metabolic models based on MAGs

CarveMe [32] was used for automatic reconstruction of genome-scale metabolic models (GEMs) for binned MAGs. The growth medium for gap-filling was anaerobic Luria–Bertani (LB) medium, as this study assumed that the oral environment was nutrient-rich and had a relatively low oxygen level, in comparison to other human body niches [33,34]. The universal bacterial template used for reconstruction, gram positive or negative, was determined based on taxonomic classification (**section 2.2**). The community-level flux balance analysis (FBA) using species metabolic interaction analysis (SMETANA) [35] was conducted to model metabolic interactions in oral bacterial communities of two different age groups. In SMETANA, the species coupling score (SCS) measures the dependency of a consumer species on a supplier species; the metabolite uptake score (MUS) measures the uptake frequency of a metabolite for a species to grow; the metabolite production score (MPS) is the ability of a species to produce a metabolite; and the SMETANA score is a multiplicative product of SCS, MUS, and MPS [35].

2.4 Quantification of oral metabolomics

Non-targeted metabolomics analysis of saliva was conducted by high-performance liquid chromatography-mass spectrometry (HPLC-MS). First, 100 μL of saliva sample was mixed with 200 μL of pre-cooled acetonitrile, followed by vortexing for 30 seconds and incubation at -20 °C for 30 minutes. The sample was then centrifuged twice at 15000 r/min at 4 °C for 10 min, and the supernatant was collected for

HPLC-MS. Quality control (QC) samples were prepared from saliva samples by pooling 10 μL aliquots from each supernatant into a single tube. In the HPLC system (Exion LC, SCIEX, USA), separation was performed using reversed phase chromatography with a Kinetex F5 column (2.1×150 mm, 2.6 μm, Phenomenex, USA). Mobile phase consisted of either water (A) or acetonitrile (B) both with 0.1% (v/v) formic acid. The elution procedure was as follows: 0-2 min, 5% B; 2-8 min, 5%-75% B; 8-13 min, 75%-98% B; 13-17 min, 98% B. The column temperature was 40 °C and the flow rate was 0.2 mL/min. In the MS system (X500R QTOF, SCIEX, USA), the data was collected by electrospray ionization (ESI, Jet Stream) in positive and negative polarity. The MS1 scan range was set to 60~1300 m/z, and information-dependent acquisition (IDA) was used. The MS2 scan range was 40-1300 m/z with dynamic background subtraction (DBS) enabled. Collision-induced dissociation was performed with a collision energy of 35±15 eV. The data was collected by SCIEX OS software, and the metabolites were identified using MExplorer Ultimate software by querying multiple databases, including HMDB [36], Metlin [37], MoNA [38], GNPS LipidBlast [39], and MS-DIAL [40]. Peak areas of detected metabolites were normalized in each sample to quantify the relative abundance levels. The origins of oral metabolites (e.g., host, microbiota) were classified by MetOrigin-2.0 [41].

2.5 Mono- and co-culture experiments of identified key oral bacteria

In the following result sections, differential abundance analysis of oral bacteria (**section 3.1**), interspecies and species-metabolite correlation analysis (**section 3.2**), QS protein annotations (**section 3.4**), and metabolic interactions inferred by community-level FBA (**section 3.5**) collectively identified *Prevotella salivae*, *Ligilactobacillus salivarius*, *Streptococcus sobrinus* as key oral bacteria whose ecological interactions contributed to oral microbiome remodelling of elderly individuals. To investigate interspecies interactions of identified key oral bacteria, this study conducted co-culture experiments for *Prevotella salivae* + *Ligilactobacillus salivarius*, *Prevotella salivae* + *Streptococcus sobrinus*, *Streptococcus sobrinus* + *Ligilactobacillus salivarius*, and *Prevotella salivae* + *Ligilactobacillus salivarius* + *Streptococcus sobrinus*, and mono-culture experiments for these three species as the control samples. In detail, *Prevotella salivae* DSM 15606 was obtained from Shanghai Microbiological Culture Collection co., Ltd (Shanghai, China), *Ligilactobacillus salivarius* DSM 20555 and *Streptococcus sobrinus* DSM 20742 were obtained from BeNa Culture Collection co., Ltd (Heibei, China). These three species were revived on columbia blood agar, BHI agar, and MRS agar respectively, with an anaerobic environment maintained using anaerobe pouch system sachets and monitored via an indicator (Hopebio, Qingdao, China). All three species were maintained in GAM Broth without additives (Hopebio, Qingdao, China) at 37 ºC until the stationary phase at an optical density at 600 nm (OD_{600}) of 0.7. Then, they were inoculated at 2% (v/v) into sterile liquid medium for dual-strain (1:1 ratio) and triple-strain (1:1:1 ratio) co-cultures. The OD_{600} measurements of co-cultures and mono-cultures were taken using a multi-mode microplate reader (FLASH SPECTRUM SuPerMax 3200, Shanghai, China). For fatty acid supplementations to mono-/co-cultures, linoleic acid (>99% purity, Macklin) was directly added to pre-sterilized broth and then re-sterilized using a 0.22 uM PES filter, stearic acid (>98% purity, Macklin) was solubilized according to the reported method [42]. Stearic and linoleic acids, both 18-carbon fatty acids

abundant in daily diet [43,44], were selected to investigate the effects of saturated and unsaturated fatty acids, given the observed up-regulation of their derivatives (i.e., cis-9,10-epoxystearic acid and hydroxy-octadecenoic acid) in elderly samples (**section 3.1**). The total bacterial inoculum count was controlled to be consistent in all culture experiments, and the number of replicates was three.

2.6 Statistical analysis of multi-omics data

The dimensionality reduction of abundance levels of oral bacteria, metabolites, gene families and metabolic pathways in metagenomes was performed using uniform manifold approximation and projection (UMAP) [45]. Differential abundance analysis was performed using PyDESeq2 [46], to find out significantly up/down-regulated oral bacteria, metabolites, and functional pathways across A and B groups. In differential abundance analysis, *P*-values were all corrected for multiple testing using the Benjamini and Hochberg method [47]. For correlation analysis, Spearman coefficients were computed for inter-bacterial and bacteria-metabolite correlations, and *P*-values of Spearman correlations were also corrected for multiple testing using the Benjamini and Hochberg method. Nodes in weighted networks were clustered using Clauset-Newman-Moore greedy modularity maximization [48] for the largest modularity, and then networks were visualized as undirected graphs by NetworkX [49] in force-directed layouts.

3. Results

3.1 Differential abundance analysis identifies key oral bacteria and metabolites

In the taste sensitivity test of 10 youth (A group) and 10 elderly (B group) individuals with no significant difference in body mass indexes or daily diet types (i.e., Mainly vegetarian, Mainly meat, Balanced) (**see Table S1 in Supplementary Materials**), all youth individuals had significantly stronger taste sensitivity (lower taste detection thresholds) than elderly individuals (**Figure 2A**). The average taste detection thresholds of youth and elderly samples were 0.51 g/L and 17.14 g/L, respectively, and the statistical power of two-sample t-test was 0.99. The UMAP-transformed taxonomic profiles and oral metabolite relative abundance levels also showed distinctive distributions for youth and elderly samples (**Figure 2BC**). In comparison to youth samples, 4 species of *Haemophilus* genus and *Fusobacterium massiliense* in elderly samples had significantly lower abundance levels, while *Bifidobacterium dentium*, *Propionibacterium acidifaciens*, *Streptococcus sobrinus/mutans*, *Mitsuokella sp. oral taxon 131*, *Ligilactobacillus salivarius*, *Prevotella salivae/multisaccharivorax*, and *Cryptobacterium curtum* had significantly higher abundance levels (**Figure 2D**). These species with significantly different abundance levels were considered as key oral bacteria. Consistently, previous studies have reported that *Bifidobacterium dentium*, *Streptococcus mutans*, *Prevotella*, and *Mitsuokella* species were correlated with taste sensitivity decline [50,51], whereas the reduction of *Haemophilus* and *Fusobacterium* species in elderly samples were most likely related to aging [52,53].

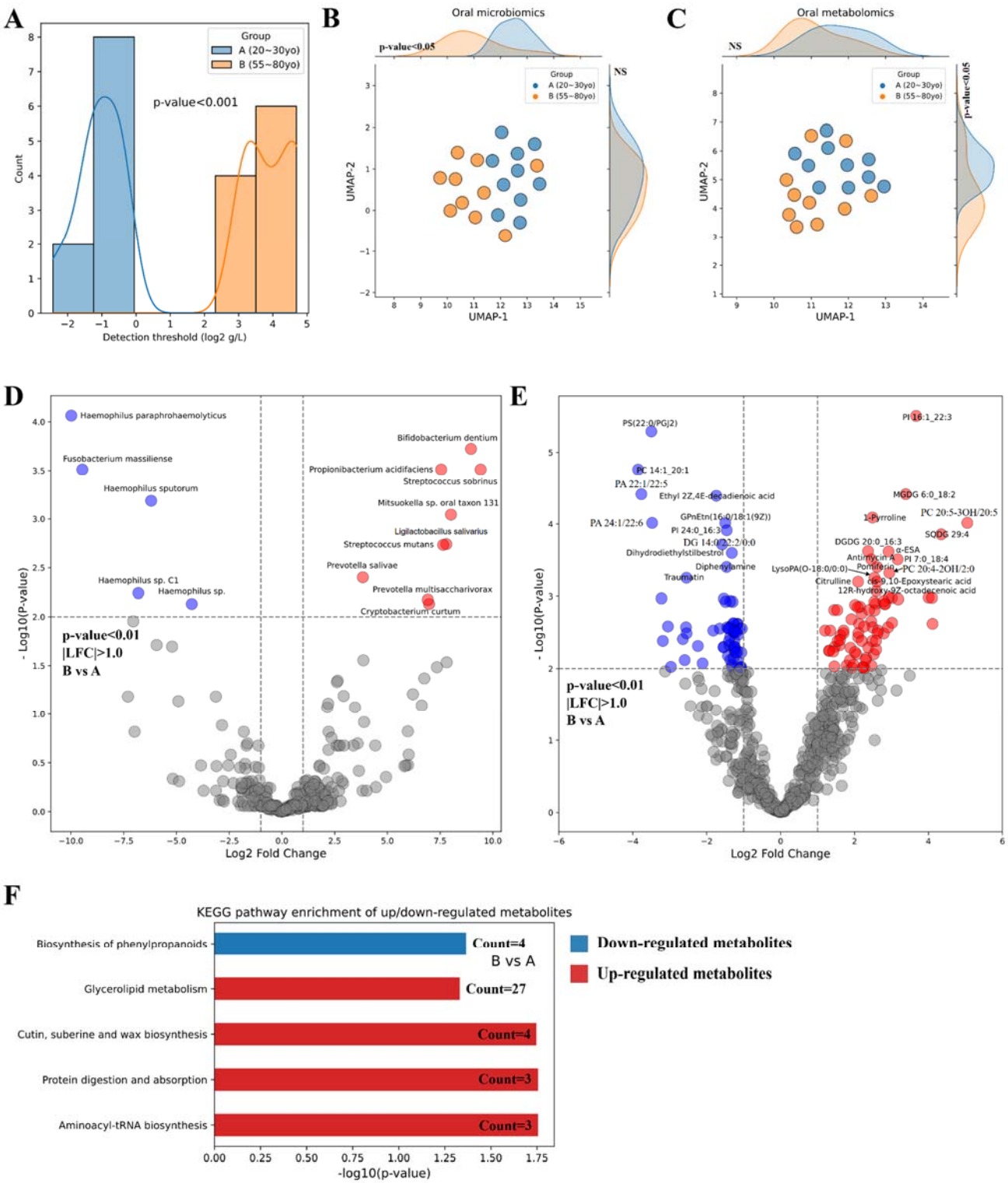


Figure 2. The analysis of taxonomic profiles of oral microbiome and oral metabolomics of youth and elderly samples. (A) The distribution of taste DTs (log2 g/L) for A and B samples. A samples: youth samples; B samples: elderly samples. (B) UMAP of taxonomic profiles of oral microbiomes of A and B samples (*P*-value < 0.05). (C) UMAP of oral metabolite abundance levels of A and B samples (*P*-value < 0.05). (D) Differential abundance analysis of genomic abundance levels of bacterial species (adjusted *P*-value < 0.01, log2-fold change>1.0). LFC: log2-fold change. (E) Differential abundance analysis of oral metabolite abundance levels (adjusted *P*-value < 0.01, log2-fold change>1.0). Only up/down-regulated metabolites with adjusted *P*-value < 0.001 were labelled. (F) KEGG pathway enrichment of significantly up/down-regulated metabolites (adjusted *P*-value < 0.05). Blue: down-regulated metabolites; Red: up-regulated metabolites.

Regarding oral metabolomics, differential abundance analysis identified 78 and 67 significantly up- and down-regulated metabolites in elderly samples versus youth samples (B vs A), respectively (**Figure 2E**).

Glycerophospholipids (e.g., PC 14:1_20:1, PI 16:1_22:3) were prevalent in both up- and down-regulated metabolites. Alpha-eleostearic acid (α-ESA), cis-9,10-epoxystearic acid, and hydroxy-octadecenoic acid were found in up-regulated metabolites with a high significance level (*P*-value < 0.001) (**Figure 2E**). The origins of oral metabolites detected in this study can be found at https://github.com/SizheQiu/OralMicroIX/data/metabolome/Metabolites_Origin.csv. The origins of α-ESA and cis-9,10-epoxystearic acid were both classified as microbiota-derived or food related, whereas that of hydroxy-octadecenoic acid was food related. Nevertheless, the origins of most significantly up-/down-regulated metabolites (e.g., glycerophospholipids such as PC 14:1_20:1) could not be distinguished as being host- or microbiota-derived. (**see Figure S2 in Supplementary Materials**). The KEGG pathway enrichment analysis showed that significantly up-regulated metabolites enriched in lipid metabolism (glycerolipid metabolism and cutin, suberine and wax biosynthesis), protein digestion and absorption, and aminoacyl-tRNA biosynthesis, while significantly down-regulated metabolites enriched in biosynthesis of phenylpropanoids (**Figure 2F**). The significantly higher levels of fatty acids and enrichment of up-regulated metabolites in lipid metabolism indicated a possible high-fat diet of elderly individuals, which was consistent with a previously reported finding that taste sensitivity decline could lead to high-fat diet [54,55]. The enrichment of up-regulated metabolites in protein digestion and absorption and aminoacyl-tRNA biosynthesis was likely caused by the up-regulation of proteolytic oral bacteria, such as *Prevotella* species *[56]* (**Figure 2D**), and aging-associated dysregulation of nitrogen metabolism [57,58]. The enrichment of down-regulated metabolites in biosynthesis of phenylpropanoids might reflect the dietary preference of elderly individuals involved in this study (e.g., a possible reduced intake of phenylpropanoid-rich fruits [59]). In essence, fatty acids were posited as key metabolites in the oral microbiome remodelling of elderly individuals.

3.2 Interspecies and species-metabolite correlations reveal ecological interactions

The correlation analysis of taxonomic profiles of youth (A) and elderly (B) samples revealed potential interspecies interactions in the oral microbiome (**Figure 3A, Figure S3 in Supplementary Materials**). *Prevotella* species had significant positive correlations with other *Prevotella* species, *Streptococcus parasanguinis/salivarius* and *Veillonella* atypica/dispar. On the other hand, *Pasteurellaceae* species, *Fusobacterium periodonticum*, and *Veillonella rogosae* had significant negative correlations with *Prevotella* and *Streptococcus* species. Two clusters of oral bacteria were observed in the force-directed weighted correlation network (**Figure 3A**). Cluster 1 mainly includes *Prevotella* and *Streptococcus* species (orange circle). Cluster 2 comprises *Haemophilus*, *Neisseria*, and *Fusobacterium* species (purple circle). Species within each cluster were positively correlated, while the two clusters were negatively correlated.

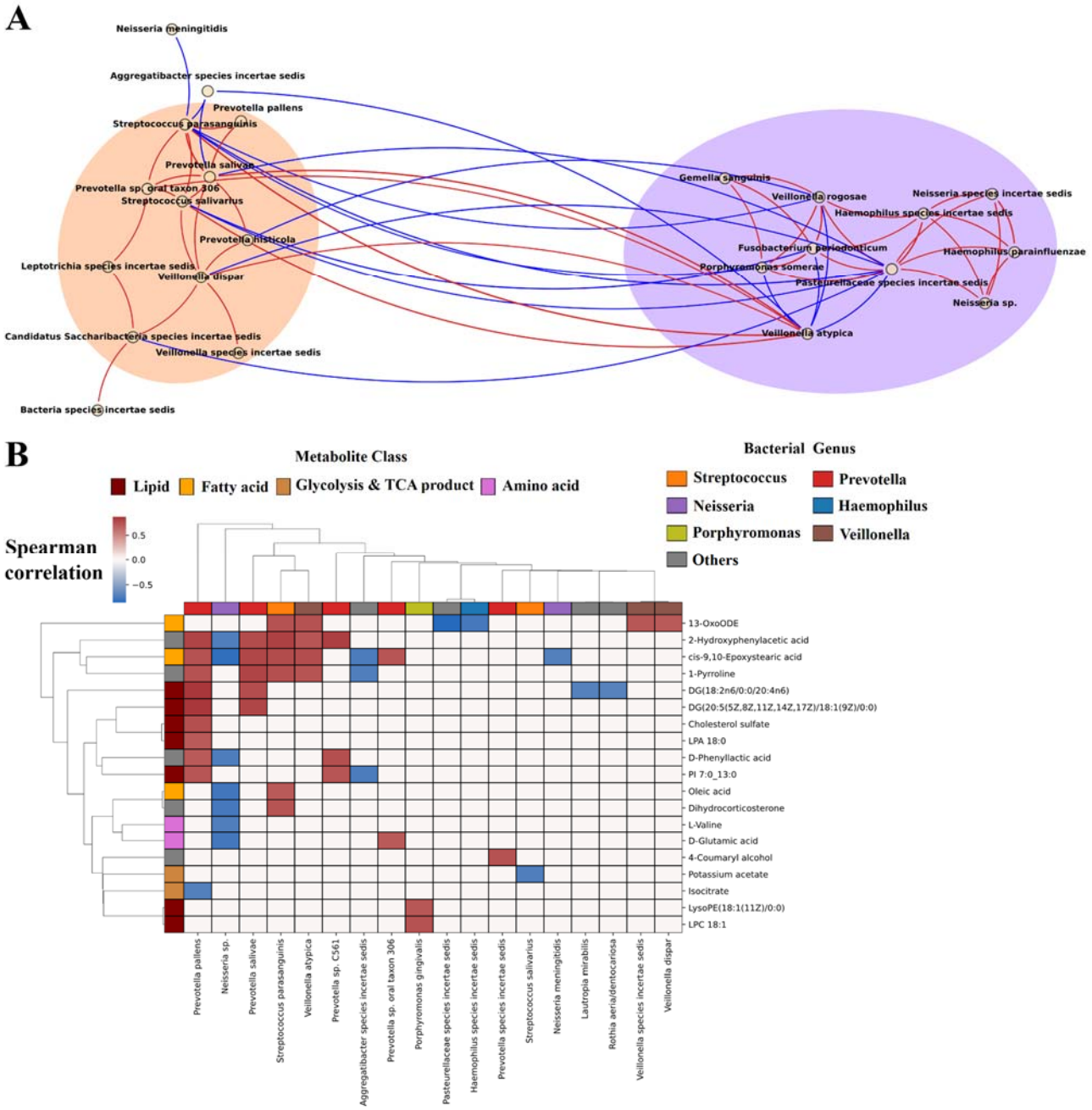


Figure 3. Correlation analysis of oral bacteria and metabolites. (A) Weighted correlation network of oral bacterial species with two major clusters labeled (*P*-value < 0.01). Blue: negative correlations; Red: positive correlations. (B) Species-metabolite spearman correlations (*P*-value < 0.05). The *P*-values in all correlation analysis were corrected for multiple testing using the Benjamini and Hochberg method.

In species-metabolite correlation analysis, *Prevotella* and *Streptococcus* species were positively correlated with fatty acids (e.g., cis-9,10-Epoxystearic acid) and lipids (e.g., LPA 18:0), while negatively correlated with acetate and isocitrate (**Figure 3B**). 13-Oxo-9Z,11E-octadecadienoic acid (13-OxoODE) was determined to be derived from food or microbiota, but the origins of the other fatty acids significantly correlated with oral bacteria were undetermined. The origin of acetate was classified as food or drug related, while the origin of isocitrate was undetermined. The significant positive correlation between D-glutamic acid and *Prevotella* sp. oral taxon 306 was possibly attributable to the proteolytic activity (**section 3.1**). Acetate and isocitrate, as products of carbon catabolism, can inhibit bacterial growth [60–62]. *Streptococcus* and *Prevotella* species are relatively more sensitive to the inhibition by acetate and isocitrate because they prefer

fast anaerobic growth in low oxidative stress and carbohydrate-rich environments [63]. Acetate is a weak acid stressor for *Streptococcus* and *Prevotella* species, as it represses carbon catabolism and causes oxidative stress [60,64]. Isocitrate inhibits isocitrate dehydrogenase activity via feedback to slow the growth of *Streptococcus* and *Prevotella* species [61,62]. On the other hand, *Haemophilus* and *Neisseria* species were negatively correlated with fatty acids. These significant correlations led us to an assumption that elevated fatty acid levels in elderly samples might be a major driving factor in the modulation of the oral microbiome (**Figure 2E**), resulting in the up-regulation of *Prevotella* and *Streptococcus* species and down-regulation of *Haemophilus* species (**Figure 2D**).

3.3 Functional pathway analysis shows the metabolic adaptation of oral microbiome

For functional analysis, gene families and metabolic pathways were quantitatively profiled for assembled metagenomes of youth (A) and elderly (B) samples. Similar to the patterns found in taxonomic profiles and oral metabolite relative abundance levels (**section 3.1)**, the abundance levels (gene copy numbers) of coding genes and metabolic pathways also demonstrated distinctive distributions for the two age groups (**Figure 4A**). Differential abundance analysis of coding genes found 129 significantly up-regulated genes and 2 significantly down-regulated genes in elderly samples, that were spermidine/putrescine ABC transporter ATP-binding protein (R0LDC5) and a response regulator of transcription (R0LF06) (**Figure 4B**). The GO annotations [65] indicated that up-regulated genes in elderly samples mainly enriched in glycolysis, phosphoenolpyruvate (PEP):sugar phosphotransferase system (PTS), IMP/CTP biosynthesis, and membrane ATP synthesis (**Figure 4C**). The analysis of metabolic pathway abundance levels based on MetaCyc [66] suggested that L-cysteine biosynthesis, isoprene biosynthesis, and Entner-Doudoroff (ED) pathway were significantly down-regulated, while glyoxylate bypass and tricarboxylic acid cycle (TCA), biosynthesis of isopropanol, L-glutamate/glutamine, taxadiene, trans-farnesol, geranylgeranyl diphosphate, and polyisoprenoid were significantly up-regulated in elderly samples (**Figure 4D**). The substrates of ED pathway and glyoxylate bypass were monosaccharides and fatty acids, respectively. Ergo, for energy metabolism of oral bacteria, the down-regulation of ED pathway, up-regulation of glyoxylate bypass, elevated fatty acid levels (**section 3.1**), and significant positive correlations between fatty acids and up-regulated oral bacteria collectively suggested an alteration in substrate preference from monosaccharides to fatty acids in elderly samples. Although the genomic abundance levels of isopropanol, trans-farnesol, and polyisoprenoid biosynthetic pathways were up-regulated (**Figure 4D**), these flavor compounds and their derivatives were not found in up-regulated oral metabolites (**section 3.1**). Therefore, their hypothesized effects on taste perception were not clearly reflected in the oral metabolomic data obtained in this study.

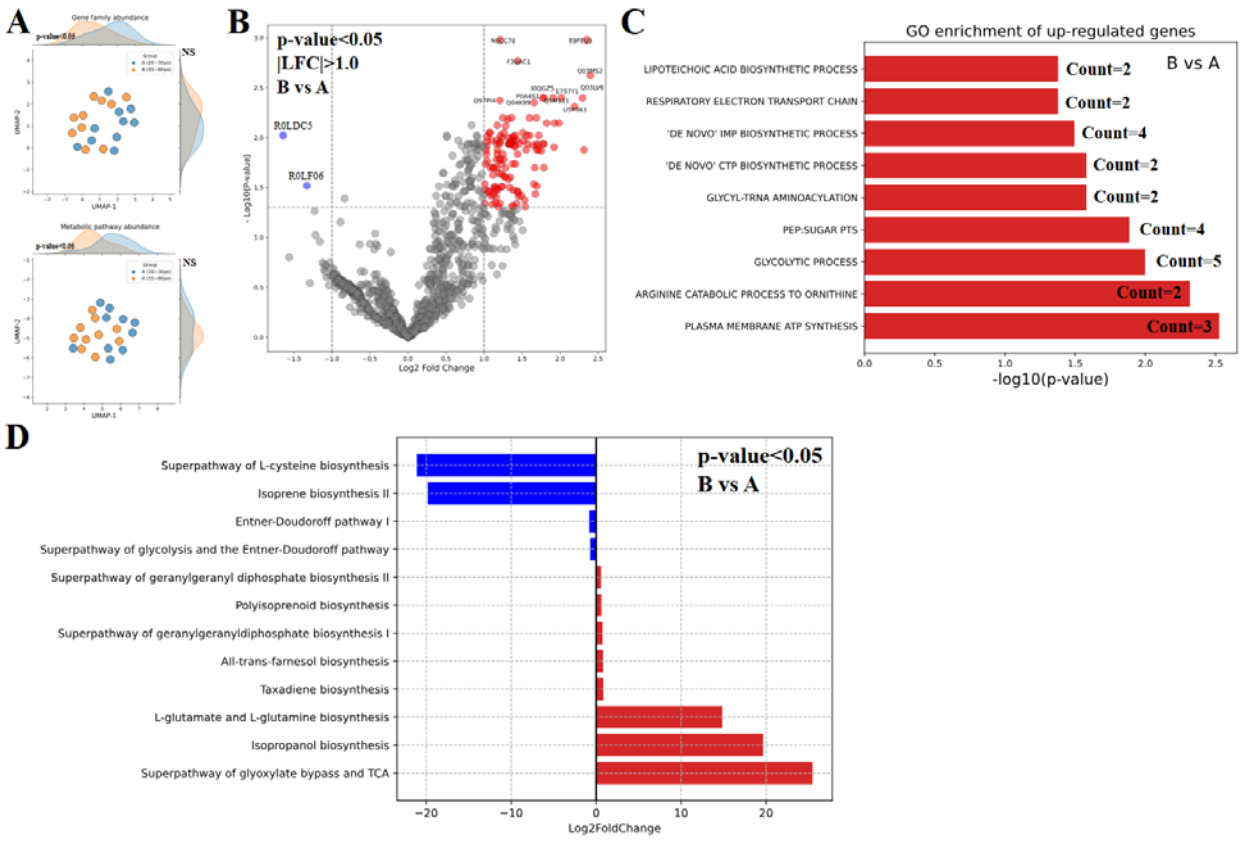


Figure 4. The analysis of gene family and functional pathway abundance in the oral metagenomes of youth and elderly samples. (A) UMAP of gene family and pathway abundance levels of samples in A and B samples (*P*-value < 0.05). A samples: youth samples; B samples: elderly samples. (B) Differential abundance analysis of coding genes (B vs A). The adjusted *P*-value and log2 fold change cutoffs are 0.05 and 1. (C) GO process enrichment of significantly up-regulated genes (adjusted *P*-value < 0.05). (D) Functional pathways of significantly high (red) and low (blue) abundance levels in B samples. The adjusted *P*-value cutoff is 0.05.

3.4 Quorum sensing protein annotations uncover cell-to-cell communication abilities of oral bacteria

After phylogenetic binning (**section 2.2**), 28 and 37 high-quality MAGs of youth (A) and elderly (B) oral microbiomes were obtained and taxonomically classified (**see Tables S3, S4, Figures S1, S2 in Supplementary Materials**). The average nucleotide identity (ANI) values of classified MAGs and template genomes were all above 95%, detailed information can be found at https://github.com/SizheQiu/OralMicroIX/data/metagenome. The annotation of quorum sensing (QS) proteins (signal molecule synthases and receptors) on MAGs revealed the cell-to-cell communication abilities of bacteria in youth and elderly oral microbiomes (**Figure 5**). Notably, noradrenaline synthase/receptor, LuxR-type receptor, and TCS (two-component systems) receptor were found in all MAGs, and therefore were excluded from further analysis. The *Prevotella* species, in both youth and elderly samples, were found to have AI-2 (autoinducer-2) and CAI-1 (cholera autoinducer-1) synthases, while around 50% of MAGs lacked those two synthases (**Figure 5A**). Almost all MAGs, except for A_bin.23 (*Metamycoplasma* genus), had CAI-1 receptors. Hence, *Prevotella* species, with relatively high abundance levels in both youth and elderly oral microbiomes (**see Figure S4 in supplementary Materials**), were inferred to serve as the major donors of AI-2 and CAI-1, which was consistent with high connectivities of *Prevotella* species in the interspecies correlation network (**Figure 3A**). Notably, A_bin.28 (*Haemophilus sputorum*), A_bin.6 (*Porphyromonas*

gingivalis), and B_bin.28 (*Streptococcus sobrinus*), which only had AI-2 synthases but not receptors, were also donors of AI-2. With respect to DSF (diffusible signaling factor)-mediated QS, *Streptococcus sobrinus* in the B community was the only species that had DSFs receptor but lacked DSFs synthase (**Figure 5B**). Therefore, it would rely on donors of DSFs, such as B_bin.1 (*Prevotella salivae*) or B_bin.32 (*Porphyromonas gingivalis*). Based on interspecies correlations, *Streptococcus sobrinus* most likely received DSFs from *Prevotella* species (**Figure 3A**). The HAQs (4-hydroxy-2-alkylquinolines) receptor and indole synthase were missing in most MAGs, suggesting that those two types of QS were inactive in oral bacterial communities studied in this work. Generally speaking, *Prevotella* species were inferred to be active in QS interactions with other oral bacteria, and their up-regulation in elderly samples (**Figure 2D**) possibly promoted the growth of its positively correlated bacteria (e.g., *Streptococcus* species), via activating biofilm formation, production of virulence factors, and antibiotic resistance, to affect oral microbiome remodelling [67,68].

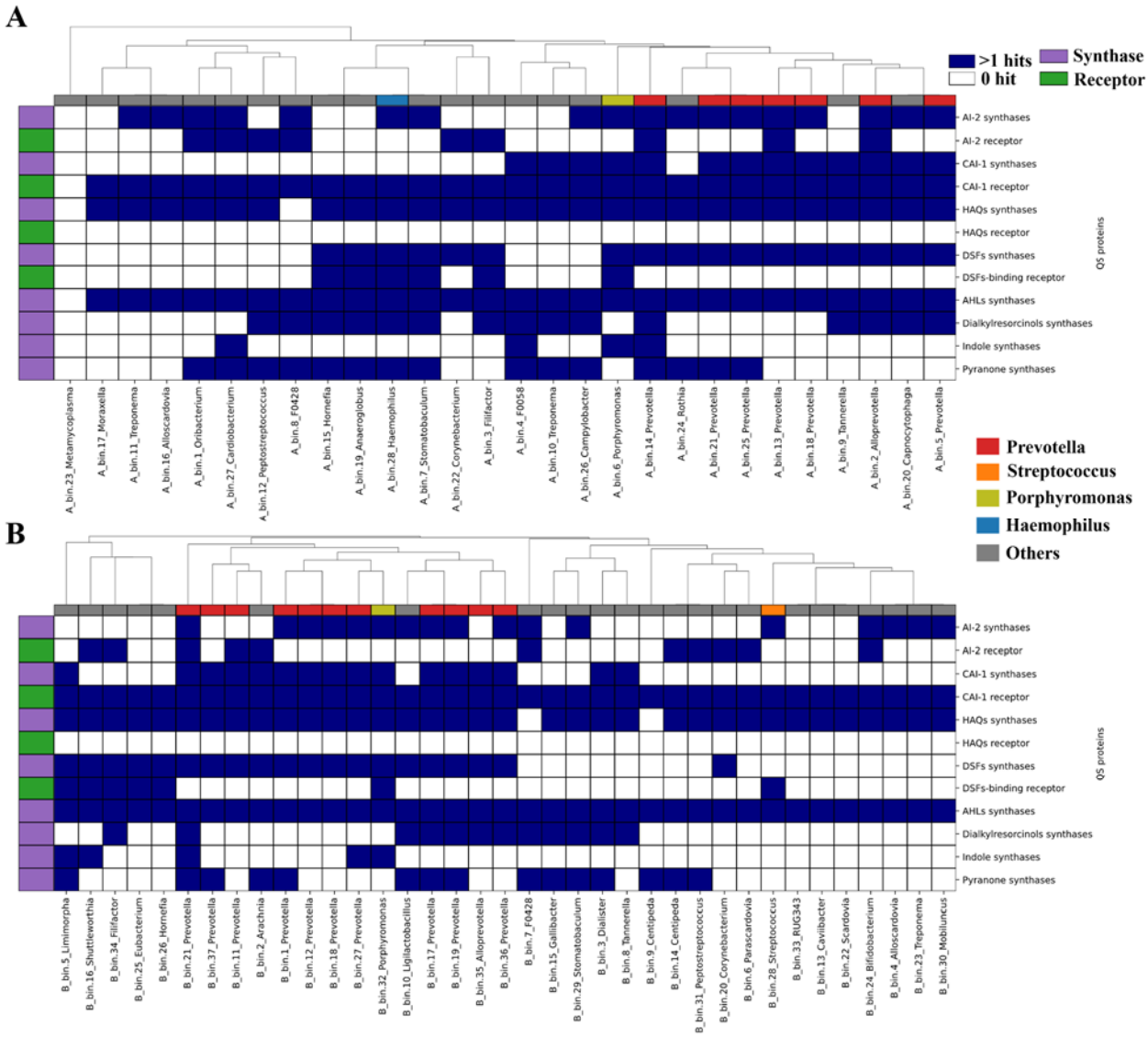


Figure 5. QS protein annotations of MAGs from youth (A) and elderly (B) oral microbiomes. The IDs of bacteria (e.g., A_bin.28 for *Haemophilus sputorum*) can be found in **Table S3, S4 in Supplementary Materials**. Navy blue: more than 1 hit in sequence alignment; White: no hit; Purple: synthase proteins; Green: receptor proteins; Red: *Prevotella*; Orange: *Streptococcus*; Yellow: *Porphyromonas*; Blue: *Haemophilus*; Grey: other bacteria genera.

3.5 Community-level metabolic modeling infers metabolic interactions among oral bacteria

To predict potential metabolic interactions of oral bacteria in youth (A) and elderly (B) samples, GEMs were reconstructed based on MAGs to perform community-level FBA (**see Figure S5 and S6 in Supplementary Materials**). In the species-coupling network of youth samples, *Oribacterium* and *Treponema* were predicted to be major consumers of nutrients, while *Cardiobacterium hominis*, *Stomatobaculum longum*, *Haemophilus sputorum*, *Prevotella histicola*, *Anaeroglobus micronuciformis*, and *Corynebacterium durum* were major suppliers of nutrients (**Figure 6A**). Specifically, *Haemophilus sputorum*, downregulated in elderly samples (**Figure 2D**), acted as a supplier of lysine (lys), arginine (arg), ammonium (nh4), and thiamin (thm) to *Oribacterium* and *Treponema* species (**Figure 6C**).

Regarding oral bacteria of elderly samples, *Prevotella* species, except *Prevotella oris*, were all predicted to be consumers, while *Stomatobaculum longum* was still a supplier of nutrients as in youth samples (**Figure 6B**). The role of *Prevotella salivae* transitioned from a supplier of amino acids, phosphate, and glycerol in youth samples to a consumer of amino acids, monosaccharides, and peptidoglycan in elderly samples (**Figure 6DE**). Correspondingly, *Streptococcus sobrinus* and *Ligilactobacillus salivarius*, up-regulated in elderly samples (**Figure 2D**), both supplied nutrients to *Prevotella salivae* (**Figure 6B**). *Streptococcus sobrinus* supplied peptidoglycan (LalaDgluMdapDala), and *Ligilactobacillus salivarius* supplied galactose (gal), which are building blocks of cell walls and polysaccharides, respectively (**Figure 6E**). *S. sobrinus* and *L. salivarius* also supplied nutrients to other *Prevotella* species, i.e., *Prevotella shahii*, *Prevotella histicola*, and *Prevotella sp905372445* (**Figure 6B, see Figure S7 in Supplementary Materials**). The simulation of metabolic fluxes predicted that the nutrient feeding from *Streptococcus sobrinus* and *Ligilactobacillus salivarius* resulted in the role transition of *Prevotella salivae*, switching from a supplier to a consumer. And this role transition likely promoted the growth of *Prevotella salivae* by alleviating its cellular metabolic burden of biomass component synthesis. Consequently, community-level metabolic modeling of oral bacteria inferred that changes in interspecies nutrient feeding patterns contributed to oral microbiome remodelling.

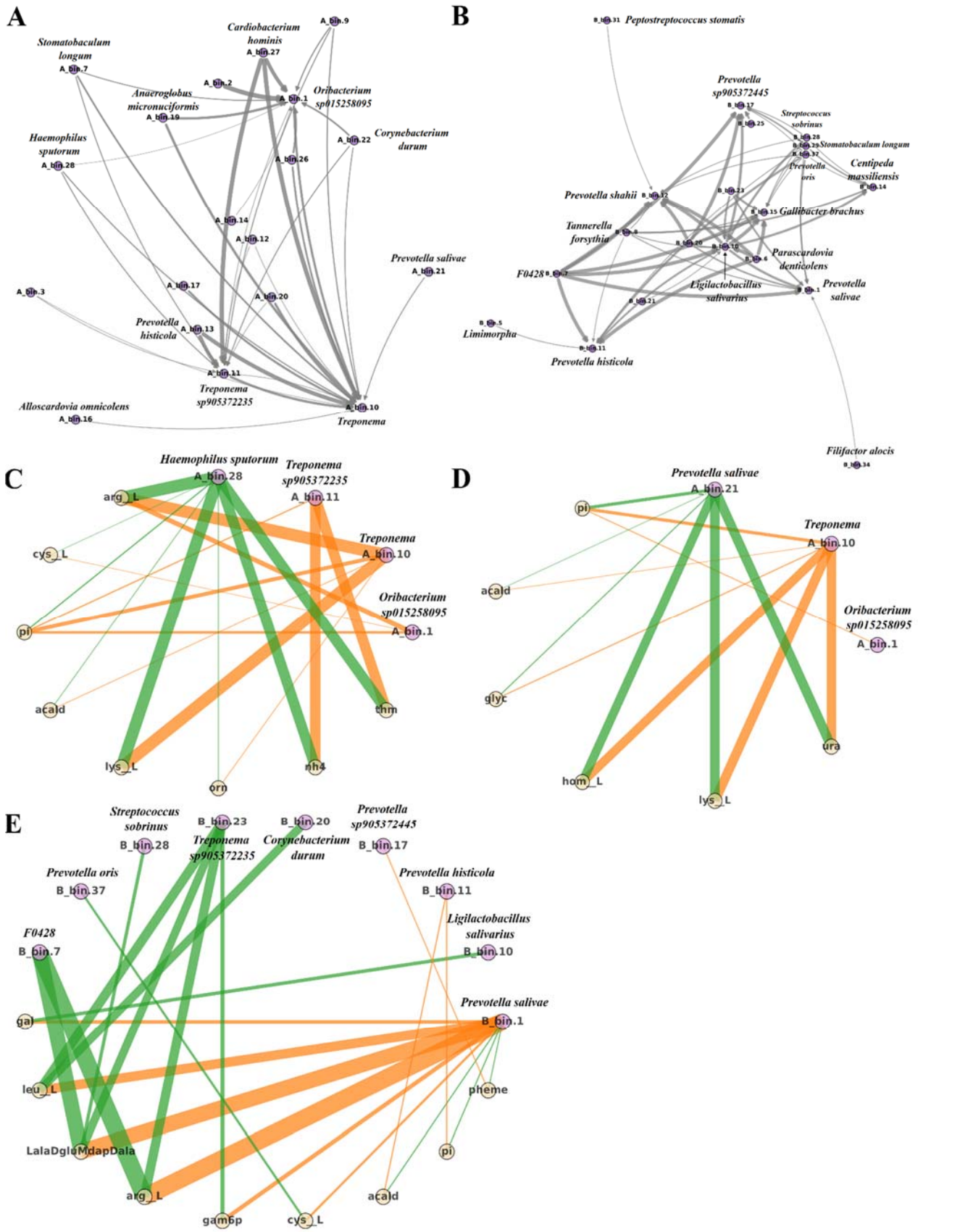


Figure 6. Results of community-level FBA of oral bacteria. (A, B) Simulated species coupling relationships of oral bacteria in youth (A) and elderly (B) samples. The widths of edges were scaled with species coupling scores (SCSs), and the directions of edges pointed from suppliers to consumers. SCS>0.1. (C-E) Simulated metabolic interactions of *Haemophilus sputorum* (C) and *Prevotella salivae* (D) in youth samples, and *Prevotella salivae* (E) in elderly samples. The widths of edges were scaled with SMETANA scores (**section 2.3**). Purple nodes: bacteria identified in phylogenetic binning; Wheat nodes: metabolites; Green edges: production; Orange edges: consumption. The IDs of bacteria (e.g., A_bin.28 for *Haemophilus sputorum*) can be found in **Table S3, S4 in Supplementary Materials**. The IDs of metabolites were adopted from the BIGG database (**see Table S5 in Supplementary Materials**).

3.6 Mono- and co-culture experiments validate inferred ecological interactions

To validate the inferred modulatory effects of fatty acids and interspecies interactions of up-regulated oral bacteria in elderly samples, mono-culture experiments of *Prevotella salivae* (P.s), *Streptococcus sobrinus* (S.s), *Ligilactobacillus salivarius* (L.s), and 2-species/3-species co-culture experiments of P.s, S.s, L.s were conducted (**Figure 7, Experiment 1&2**). Linoleic and stearic acids, as representative unsaturated and saturated fatty acids, were added to mono-/co-cultures at concentrations of 0, 0.025, and 0.05 mM. As the initial cell concentrations (OD600) of all mono-/co-cultures were the same, OD600=0.1, the OD600 values at different time points could be directly used to quantify average growth rates. With the increase of linoleic acid concentration from 0 to 0.05 mM, the average growth rates of P. s. and P. s+S. s+L. s increased significantly, while the average growth rates of S. s and L. s showed no significant changes (**Figure 7A**). On the other hand, stearic acid activated the growth of S.s and L.s, but had little effect on P.s (**Figure 7B**). In a nutshell, the inferred role of fatty acids as key drivers in remodelling the oral microbiome were experimentally validated.

Next, the growth rates of mono-cultures and 2-species/3-species co-cultures were compared to examine the inferred interspecies interactions of P.s, S.s, and L.s (**Figure 7C-F**). The 2-species co-cultures of P.s+S.s and P.s+L.s, and 3-species co-culture of P.s+S.s+L.s all had significantly faster growth rates than mono-cultures (P.s, S.s, and L.s) (**Figure 7CDF**), validating that S.s and L.s can promote the growth of P.s (**section 3.5**) as well as suggesting that P.s can benefit the growth of S.s and L.s, possibly via enhanced QS activity (**section 3.4**). Nevertheless, the relationship between S.s and L.s was unclear, as the growth rates of L.s+S.s and S.s did not have significant differences (**Figure 7E**). In short, the commensalistic interactions of S.s and L.s with P.s were experimentally validated.

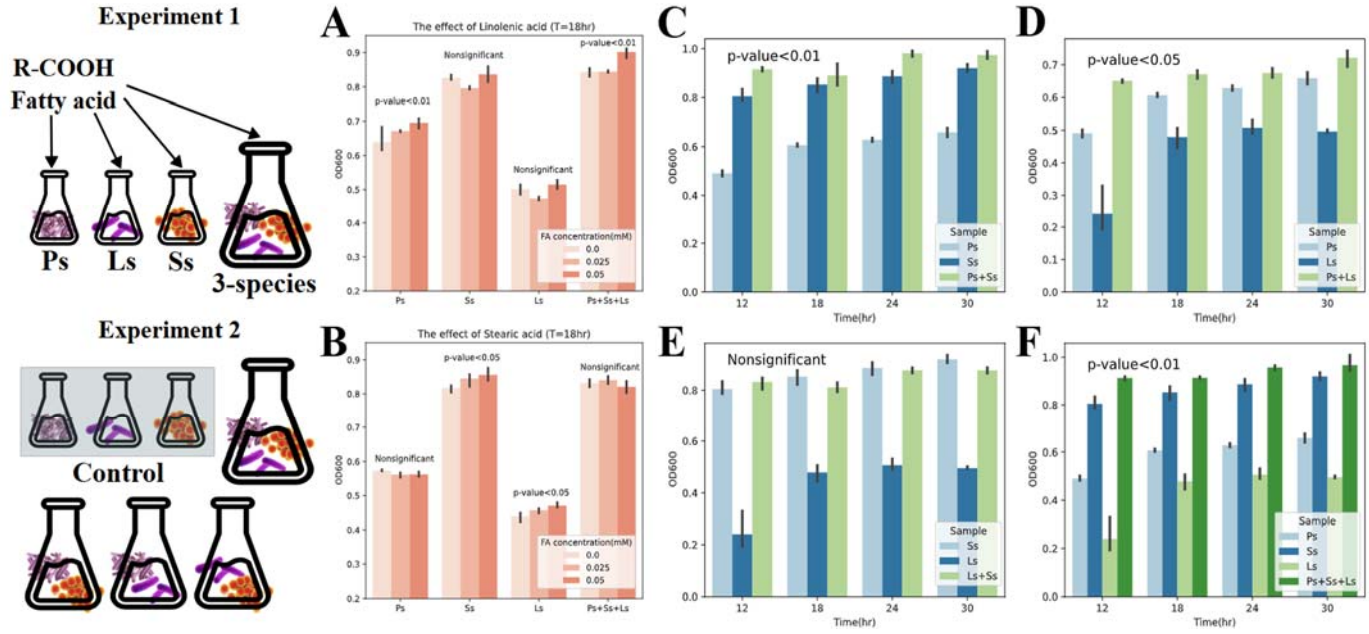


Figure 7. The cell concentrations (OD600) of mono-cultures and co-cultures of *Prevotella salivae* (P.s), *Streptococcus sobrinus* (S.s), and *Ligilactobacillus salivarius* (L.s) under different conditions. (A) OD600 at T=18hr of P.s, S.s, L.s, and P.s+S.s+L.s under different concentrations of linoleic acid (0, 0.025, 0.05 mM). (B) OD600 at T=18hr of P.s, S.s, L.s, and P.s+L.s+S.s under different concentrations of stearic acid (0, 0.025, 0.05 mM). (C) OD600 of P.s, S.s, and P.s+S.s at T=12, 18, 24, 30hr. (D) OD600 of P.s, L.s, and P.s+L.s at T=12, 18, 24, 30hr. (E) OD600 of L.s, S.s, and L.s+S.s at T=12, 18, 24, 30hr. (F) OD600 of P.s, S.s, L.s, and P.s+S.s+L.s at T=12, 18, 24, 30hr. The initial OD600 were all 0.1.

4. Discussion

Focusing on the complicated interconnection of aging-induced taste sensitivity decline and oral microbiome, this study managed to provide a mechanistic depiction of how the former remodels the latter through multi-omics analysis of oral samples from a case study cohort comprising youth and elderly individuals in Fangshan district, Beijing, China. Regarding the key oral bacteria, *Prevotella salivae*, *Streptococcus sobrinus*, *Ligilactobacillus salivarius*, and other 6 species were found to have significantly higher abundance levels in elderly samples (**section 3.1**). With respect to key metabolites, species-metabolite correlations and functional pathway analysis of the oral metagenome suggested that elevated levels of fatty acids (e.g., cis-9,10-epoxystearic acid) in elderly samples with low taste sensitivity (**section 3.1**) modulated the oral microbiome composition by switching the substrate preference of energy metabolism from monosaccharides to fatty acids (**section 3.2/3.3**). Correspondingly, the modulatory effects of saturated and unsaturated fatty acids on oral bacteria were validated in both mono- and co-cultures of identified key oral bacteria (**section 3.6**). Additionally, up-regulated *Prevotella* species in elderly samples possibly affected oral microbiome remodelling via active QS interactions with other oral bacteria (**section 3.4**). Furthermore, community-level genome-scale metabolic modeling and co-culture experiments suggested that the nutrient feeding from *Streptococcus sobrinus* and *Ligilactobacillus salivarius*, up-regulated in elderly samples, promoted the growth of *Prevotella salivae* and contributed to oral microbiome remodelling (**section 3.5/3.6**).

Despite the novel insights presented above, several limitations remained to be discussed. Due to resource limitations, this study was confined to 20 participants from Fangshan District, Beijing, China, which might restrict the generalizability of the findings. Incorporating more geographically diverse populations in future research would help address this limitation. In functional pathway analysis, this study quantified the expression levels of metabolic pathways with gene copy numbers (**section 3.3**), which was unable to account for transcriptional and translational regulations, although gene copy numbers have high correlations with transcription levels [69,70]. Meta-transcriptomics analysis of the oral microbiome of two age groups will provide more accurate quantification of functional pathway expression levels. Regarding non-targeted metabolomics (**section 2.4**), the annotations of certain metabolites remained preliminary, despite its capacity for broad and unbiased biomarker analysis. By contrast, targeted metabolomics using isotopically labeled or external standards allows precise quantification of key metabolite biomarkers. Besides, the oral metabolomics analysis presented in this study did not investigate the relationship between oral metabolites and taste sensitivity due to the difficulty of annotating tastants. For example, this study failed to interpret the roles of glycerolipids, present in both up/down-regulated metabolites in B samples, as the structures of detected glycerolipids were diverse and complicated (**section 3.3**). As a result, this study contributed little to explaining the influence of oral bacteria and metabolites on taste sensitivity. The further development of tastant databases, such as FlavorDB [71] and ChemTastesDB [72], can potentially resolve this limitation. Another important limitation in the oral metabolomics analysis was the inability to determine the origins of many oral metabolites as host- or microbiota-derived (e.g., isocitrate), potentially confounding the species-metabolite

correlation analysis. In vitro metabolomics of oral bacteria could avoid the interference of host metabolism, but accurately replicating the oral environment for isolated oral bacteria is challenging and some oral bacteria are non-culturable [73].

In conclusion, this multi-omics study, in spite of several limitations, successfully elucidated how aging-induced taste sensitivity decline remodels the oral microbiome by deciphering the ecological interactions of key oral bacteria (e.g., *Prevotella salivae*) and metabolites (e.g., fatty acids such as cis-9,10-epoxystearic acid). As envisaged, such mechanistic insights into the adaptation of the oral microbiome can contribute to the development of novel strategies to mitigate oral dysbiosis, eventually benefiting the health of elderly individuals.

Conflict of Interest Statement

The authors declare that there is no conflict of interest.

Data availability statement

The code and data are openly available at https://github.com/SizheQiu/OralMicroIX and supplementary information. The raw sequencing reads were deposited into the NCBI Sequence Read Archive (SRA) database (Accession Number: PRJNA1206801).

References

[1] M. Padeiro, P. Santana, M. Grant, Global aging and health determinants in a changing world, in: Aging, Elsevier, 2023: pp. 3–30. https://doi.org/10.1016/b978-0-12-823761-8.00021-5.

[2] S. Jeon, Y. Kim, S. Min, M. Song, S. Son, S. Lee, Taste sensitivity of elderly people is associated with quality of life and inadequate dietary intake, Nutrients 13 (2021) 1693. https://doi.org/10.3390/nu13051693.

[3] G. Sergi, G. Bano, S. Pizzato, N. Veronese, E. Manzato, Taste loss in the elderly: Possible implications for dietary habits, Crit. Rev. Food Sci. Nutr. 57 (2017) 3684–3689. https://doi.org/10.1080/10408398.2016.1160208.

[4] S. Santonocito, A. Giudice, A. Polizzi, G. Troiano, E.M. Merlo, R. Sclafani, G. Grosso, G. Isola, A cross-talk between diet and the oral microbiome: Balance of nutrition on inflammation and immune system's response during periodontitis, Nutrients 14 (2022) 2426. https://doi.org/10.3390/nu14122426.

[5] A. Imoscopi, E.M. Inelmen, G. Sergi, F. Miotto, E. Manzato, Taste loss in the elderly: epidemiology, causes and consequences, Aging Clin. Exp. Res. 24 (2012) 570–579. https://doi.org/10.3275/8520.

[6] G. Turconi, M. Rossi, C. Roggi, L. Maccarini, Nutritional status, dietary habits, nutritional knowledge and self-care assessment in a group of older adults attending community centres in Pavia, Northern Italy, J. Hum. Nutr. Diet. 26 (2013) 48–55. https://doi.org/10.1111/j.1365-277X.2012.01289.x.

[7] C. Mameli, C. Cattaneo, S. Panelli, F. Comandatore, A. Sangiorgio, G. Bedogni, C. Bandi, G. Zuccotti, E. Pagliarini, Taste perception and oral microbiota are associated with obesity in children and adolescents, PLoS One 14 (2019) e0221656. https://doi.org/10.1371/journal.pone.0221656.

[8] C. Cattaneo, G. Gargari, R. Koirala, M. Laureati, P. Riso, S. Guglielmetti, E. Pagliarini, New insights into the relationship between taste perception and oral microbiota composition, Sci. Rep. 9 (2019) 3549. https://doi.org/10.1038/s41598-019-40374-3.

[9] A. Esberg, S. Haworth, P. Hasslöf, P. Lif Holgerson, I. Johansson, Oral Microbiota profile associates with sugar intake and taste preference genes, Nutrients 12 (2020) 681. https://doi.org/10.3390/nu12030681.

[10] I. Rud, V.L. Almli, I. Berget, D. Tzimorotas, P. Varela, Taste perception and oral microbiota: recent advances and future perspectives, Curr. Opin. Food Sci. 51 (2023) 101030. https://doi.org/10.1016/j.cofs.2023.101030.

[11] H. Licandro, C. Truntzer, S. Fromentin, C. Morabito, B. Quinquis, N. Pons, C. Martin, H.M. Blottière, E. Neyraud, The bacterial species profiles of the lingual and salivary microbiota differ with basic tastes sensitivity in human, Sci. Rep. 13 (2023) 20339. https://doi.org/10.1038/s41598-023-47636-1.

[12] R. Barragán, O. Coltell, O. Portolés, E.M. Asensio, J.V. Sorlí, C. Ortega-Azorín, J.I. González, C. Sáiz, R. Fernández-Carrión, J.M. Ordovas, D. Corella, Bitter, sweet, salty, sour and umami taste perception decreases with age: Sex-specific analysis, modulation by genetic variants and taste-preference associations in 18 to 80 year-old subjects, Nutrients 10 (2018) 1539. https://doi.org/10.3390/nu10101539.

[13] Y. Zhou, C.-S. Tse, Sweet taste brings happiness, but happiness does not taste sweet: the unidirectionality of taste-emotion metaphoric association, J. Cogn. Psychol. (Hove) 34 (2022) 339–361. https://doi.org/10.1080/20445911.2021.2020797.

[14] P. Prinz, Sweetness preference and its impact on energy intake and body weight - a review of evidence, Front. Nutr. 10 (2023) 1289028. https://doi.org/10.3389/fnut.2023.1289028.

[15] H.T. Lawless, H. Heymann, Sensory evaluation of food: Principles and practices, 2nd ed., Springer, New York, NY, 2010. https://doi.org/10.1007/978-1-4419-6488-5.

[16] ISO 3972:2011, ISO (2023). https://www.iso.org/standard/50110.html (accessed March 18, 2025).

[17] D. Guedes, M. Prada, M.V. Garrido, I. Caeiro, C. Simões, E. Lamy, Sensitive to music? Examining the crossmodal effect of audition on sweet taste sensitivity, Food Res. Int. 173 (2023) 113256. https://doi.org/10.1016/j.foodres.2023.113256.

[18] D. Li, R. Luo, C.-M. Liu, C.-M. Leung, H.-F. Ting, K. Sadakane, H. Yamashita, T.-W. Lam, MEGAHIT v1.0: A fast and scalable metagenome assembler driven by advanced methodologies and community practices, Methods 102 (2016) 3–11. https://doi.org/10.1016/j.ymeth.2016.02.020.

[19] H.-J. Ruscheweyh, A. Milanese, L. Paoli, A. Sintsova, D.R. Mende, G. Zeller, S. Sunagawa, mOTUs: Profiling Taxonomic Composition, Transcriptional Activity and Strain Populations of Microbial Communities, Curr Protoc 1 (2021) e218. https://doi.org/10.1002/cpz1.218.

[20] D. Kang, F. Li, E.S. Kirton, A. Thomas, R.S. Egan, H. An, Z. Wang, MetaBAT 2: an adaptive binning algorithm for robust and efficient genome reconstruction from metagenome assemblies, (2019). https://doi.org/10.7717/peerj.7359.

[21] Y.-W. Wu, B.A. Simmons, S.W. Singer, MaxBin 2.0: an automated binning algorithm to recover genomes from multiple metagenomic datasets, Bioinformatics 32 (2016) 605–607. https://doi.org/10.1093/bioinformatics/btv638.

[22] J. Alneberg, B.S. Bjarnason, I. de Bruijn, M. Schirmer, J. Quick, U.Z. Ijaz, N.J. Loman, A.F. Andersson, C. Quince, CONCOCT: Clustering cONtigs on COverage and ComposiTion, arXiv [q-bio.GN] (2013). http://arxiv.org/abs/1312.4038.

[23] G.V. Uritskiy, J. DiRuggiero, J. Taylor, MetaWRAP—a flexible pipeline for genome-resolved metagenomic data analysis, Microbiome 6 (2018) 1–13. https://doi.org/10.1186/s40168-018-0541-1.

[24] P.-A. Chaumeil, A.J. Mussig, P. Hugenholtz, D.H. Parks, GTDB-Tk: a toolkit to classify genomes with the Genome Taxonomy Database, Bioinformatics (2019). https://doi.org/10.1093/bioinformatics/btz848.

[25] R. Patro, G. Duggal, M.I. Love, R.A. Irizarry, C. Kingsford, Salmon provides fast and bias-aware quantification of transcript expression, Nat. Methods 14 (2017) 417–419. https://doi.org/10.1038/nmeth.4197.

[26] D. Hyatt, G.-L. Chen, P.F. Locascio, M.L. Land, F.W. Larimer, L.J. Hauser, Prodigal: prokaryotic gene recognition and translation initiation site identification, BMC Bioinformatics 11 (2010) 119. https://doi.org/10.1186/1471-2105-11-119.

[27] F. Beghini, L.J. McIver, A. Blanco-Míguez, L. Dubois, F. Asnicar, S. Maharjan, A. Mailyan, P. Manghi, M. Scholz, A.M. Thomas, M. Valles-Colomer, G. Weingart, Y. Zhang, M. Zolfo, C. Huttenhower, E.A. Franzosa, N. Segata, Integrating taxonomic, functional, and strain-level profiling of diverse microbial communities with bioBakery 3, Elife 10 (2021). https://doi.org/10.7554/eLife.65088.

[28] C. Camacho, G. Coulouris, V. Avagyan, N. Ma, J. Papadopoulos, K. Bealer, T.L. Madden, BLAST+: architecture and applications, BMC Bioinformatics 10 (2009) 421. https://doi.org/10.1186/1471-2105-10-421.

[29] A. Rajput, K. Kaur, M. Kumar, SigMol: repertoire of quorum sensing signaling molecules in prokaryotes, Nucleic Acids Res. 44 (2016) D634–9. https://doi.org/10.1093/nar/gkv1076.

[30] E. Wynendaele, A. Bronselaer, J. Nielandt, M. D'Hondt, S. Stalmans, N. Bracke, F. Verbeke, C. Van De Wiele, G. De Tré, B. De Spiegeleer, Quorumpeps database: chemical space, microbial origin and functionality of quorum sensing peptides, Nucleic Acids Res. 41 (2013) D655–9. https://doi.org/10.1093/nar/gks1137.

[31] S. Wu, J. Feng, C. Liu, H. Wu, Z. Qiu, J. Ge, S. Sun, X. Hong, Y. Li, X. Wang, A. Yang, F. Guo, J. Qiao, Machine learning aided construction of the quorum sensing communication network for human gut microbiota, Nat. Commun. 13 (2022) 3079. https://doi.org/10.1038/s41467-022-30741-6.

[32] D. Machado, S. Andrejev, M. Tramontano, K.R. Patil, Fast automated reconstruction of genome-scale metabolic models for microbial species and communities, Nucleic Acids Res. 46 (2018) 7542–7553. https://doi.org/10.1093/nar/gky537.

[33] S.M. Faran Ali, F. Tanwir, Oral microbial habitat a dynamic entity, J. Oral Biol. Craniofac. Res. 2 (2012) 181–187. https://doi.org/10.1016/j.jobcr.2012.07.001.

[34] A. Abass, T. Okano, K. Boonyaleka, R. Kinoshita-Daitoku, S. Yamaoka, H. Ashida, T. Suzuki, Effect of low oxygen concentration on activation of inflammation by Helicobacter pylori, Biochem. Biophys. Res. Commun. 560 (2021) 179–185. https://doi.org/10.1016/j.bbrc.2021.04.123.

[35] A. Zelezniak, S. Andrejev, O. Ponomarova, D.R. Mende, P. Bork, K.R. Patil, Metabolic dependencies drive species co-occurrence in diverse microbial communities, Proc. Natl. Acad. Sci. U. S. A. 112 (2015) 6449–6454. https://doi.org/10.1073/pnas.1421834112.

[36] D.S. Wishart, A. Guo, E. Oler, F. Wang, A. Anjum, H. Peters, R. Dizon, Z. Sayeeda, S. Tian, B.L. Lee, M. Berjanskii, R. Mah, M. Yamamoto, J. Jovel, C. Torres-Calzada, M. Hiebert-Giesbrecht, V.W. Lui, D. Varshavi, D. Varshavi, D. Allen, D. Arndt, N. Khetarpal, A. Sivakumaran, K. Harford, S. Sanford, K. Yee, X. Cao, Z. Budinski, J. Liigand, L. Zhang, J. Zheng, R. Mandal, N. Karu, M. Dambrova, H.B. Schiöth, R. Greiner, V. Gautam, HMDB 5.0: The Human Metabolome Database for 2022, Nucleic Acids Res. 50 (2022) D622–D631. https://doi.org/10.1093/nar/gkab1062.

[37] C.A. Smith, G. O'Maille, E.J. Want, C. Qin, S.A. Trauger, T.R. Brandon, D.E. Custodio, R. Abagyan, G. Siuzdak, METLIN: a metabolite mass spectral database, Ther. Drug Monit. 27 (2005) 747–751. https://doi.org/10.1097/01.ftd.0000179845.53213.39.

[38] H. Horai, M. Arita, S. Kanaya, Y. Nihei, T. Ikeda, K. Suwa, Y. Ojima, K. Tanaka, S. Tanaka, K. Aoshima, Y. Oda, Y. Kakazu, M. Kusano, T. Tohge, F. Matsuda, Y. Sawada, M.Y. Hirai, H. Nakanishi, K. Ikeda, N. Akimoto, T. Maoka, H. Takahashi, T. Ara, N. Sakurai, H. Suzuki, D. Shibata, S. Neumann, T. Iida, K. Tanaka, K. Funatsu, F. Matsuura, T. Soga, R. Taguchi, K. Saito, T. Nishioka, MassBank: a public repository for sharing mass spectral data for life sciences, J. Mass Spectrom. 45 (2010) 703–714. https://doi.org/10.1002/jms.1777.

[39] M. Wang, J.J. Carver, V.V. Phelan, L.M. Sanchez, N. Garg, Y. Peng, D.D. Nguyen, J. Watrous, C.A. Kapono, T. Luzzatto-Knaan, C. Porto, A. Bouslimani, A.V. Melnik, M.J. Meehan, W.-T. Liu, M. Crüsemann, P.D. Boudreau, E. Esquenazi, M. Sandoval-Calderón, R.D. Kersten, L.A. Pace, R.A. Quinn, K.R. Duncan, C.-C. Hsu, D.J. Floros, R.G. Gavilan, K. Kleigrewe, T. Northen, R.J. Dutton, D. Parrot, E.E. Carlson, B. Aigle, C.F. Michelsen, L. Jelsbak, C. Sohlenkamp, P. Pevzner, A. Edlund, J. McLean, J. Piel, B.T. Murphy, L. Gerwick, C.-C. Liaw, Y.-L. Yang, H.-U. Humpf, M. Maansson, R.A. Keyzers, A.C. Sims, A.R. Johnson, A.M. Sidebottom, B.E. Sedio, A. Klitgaard, C.B. Larson, C.A.B. P, D. Torres-Mendoza, D.J. Gonzalez, D.B. Silva, L.M. Marques, D.P. Demarque, E. Pociute, E.C. O'Neill, E. Briand, E.J.N. Helfrich, E.A. Granatosky, E. Glukhov, F. Ryffel, H. Houson, H. Mohimani, J.J. Kharbush, Y. Zeng, J.A. Vorholt, K.L. Kurita, P. Charusanti, K.L. McPhail, K.F. Nielsen, L. Vuong, M. Elfeki, M.F. Traxler, N. Engene, N. Koyama, O.B. Vining, R. Baric, R.R. Silva, S.J. Mascuch, S. Tomasi, S. Jenkins, V. Macherla, T. Hoffman, V. Agarwal, P.G. Williams, J. Dai, R. Neupane, J. Gurr, A.M.C. Rodríguez, A. Lamsa, C. Zhang, K. Dorrestein, B.M. Duggan, J. Almaliti, P.-M. Allard, P. Phapale, L.-F. Nothias, T. Alexandrov, M. Litaudon, J.-L. Wolfender, J.E. Kyle, T.O. Metz, T. Peryea, D.-T. Nguyen, D. VanLeer, P. Shinn, A. Jadhav, R. Müller, K.M. Waters, W. Shi, X. Liu, L. Zhang, R. Knight, P.R. Jensen, B.O. Palsson, K. Pogliano, R.G. Linington, M. Gutiérrez, N.P. Lopes, W.H. Gerwick, B.S. Moore, P.C. Dorrestein, N. Bandeira, Sharing and community curation of mass spectrometry data with Global Natural Products Social Molecular Networking, Nat. Biotechnol. 34 (2016) 828–837. https://doi.org/10.1038/nbt.3597.

[40] H. Tsugawa, T. Cajka, T. Kind, Y. Ma, B. Higgins, K. Ikeda, M. Kanazawa, J. VanderGheynst, O. Fiehn, M. Arita, MS-DIAL: data-independent MS/MS deconvolution for comprehensive metabolome analysis, Nat. Methods 12 (2015) 523–526. https://doi.org/10.1038/nmeth.3393.

[41] G. Yu, C. Xu, D. Zhang, F. Ju, Y. Ni, MetOrigin: Discriminating the origins of microbial metabolites for integrative analysis of the gut microbiome and metabolome, Imeta 1 (2022) e10. https://doi.org/10.1002/imt2.10.

[42] S. Huang, J.M. Rutkowsky, R.G. Snodgrass, K.D. Ono-Moore, D.A. Schneider, J.W. Newman, S.H. Adams, D.H. Hwang, Saturated fatty acids activate TLR-mediated proinflammatory signaling pathways, J. Lipid Res. 53 (2012) 2002–2013. https://doi.org/10.1194/jlr.D029546.

[43] J.E. Hunter, J. Zhang, P.M. Kris-Etherton, Cardiovascular disease risk of dietary stearic acid compared with trans, other saturated, and unsaturated fatty acids: a systematic review, Am. J. Clin. Nutr. 91 (2010) 46–63. https://doi.org/10.3945/ajcn.2009.27661.

[44] A.Y. Taha, Linoleic acid-good or bad for the brain?, Npj Sci. Food 4 (2020) 1. https://doi.org/10.1038/s41538-019-0061-9.

[45] L. McInnes, J. Healy, J. Melville, UMAP: Uniform Manifold Approximation and Projection for Dimension Reduction, arXiv [stat.ML] (2018). https://doi.org/10.48550/ARXIV.1802.03426.

[46] B. Muzellec, M. Teleńczuk, V. Cabeli, M. Andreux, PyDESeq2: a python package for bulk RNA-seq differential expression analysis, Bioinformatics 39 (2023). https://doi.org/10.1093/bioinformatics/btad547.

[47] Y. Benjamini, Y. Hochberg, Controlling the false discovery rate: A practical and powerful approach to multiple testing, J. R. Stat. Soc. Series B Stat. Methodol. 57 (1995) 289–300. https://doi.org/10.1111/j.2517-6161.1995.tb02031.x.

[48] A. Clauset, M.E.J. Newman, C. Moore, Finding community structure in very large networks, Phys. Rev. E Stat. Nonlin. Soft Matter Phys. 70 (2004) 066111. https://doi.org/10.1103/PhysRevE.70.066111.

[49] A. Hagberg, P.J. Swart, D.A. Schult, Exploring network structure, dynamics, and function using NetworkX, Los Alamos National Laboratory (LANL), Los Alamos, NM (United States), 2008. https://www.osti.gov/biblio/960616 (accessed July 26, 2023).

[50] A. Jurczak, M. Jamka-Kasprzyk, Z. Bębenek, M. Staszczyk, P. Jagielski, D. Kościelniak, I. Gregorczyk-Maga, I. Kołodziej, M. Kępisty, M. Kukurba-Setkowicz, A. Bryll, W. Krzyściak, Differences in sweet taste perception and its association with the streptococcus mutans cariogenic profile in preschool children with caries, Nutrients 12 (2020) 2592. https://doi.org/10.3390/nu12092592.

[51] P.C. López-Dávalos, T. Requena, M.Á. Pozo-Bayón, C. Muñoz-González, Decreased retronasal olfaction and taste perception in obesity are related to saliva biochemical and microbiota composition, Food Res. Int. 167 (2023) 112660. https://doi.org/10.1016/j.foodres.2023.112660.

[52] A. Kazarina, J. Kuzmicka, S. Bortkevica, P. Zayakin, J. Kimsis, V. Igumnova, D. Sadovska, L. Freimane, A. Kivrane, A. Namina, V. Capligina, A. Poksane, R. Ranka, Oral microbiome variations related to ageing: possible implications beyond oral health, Arch. Microbiol. 205 (2023) 116. https://doi.org/10.1007/s00203-023-03464-5.

[53] L. Guo, J. Zhou, F. Xie, Q. Lang, Y. Xu, L. Chen, Z. Xue, Y. Mao, R. Wang, The profile of oral microbiome in Chinese elderly population associated with aging and systemic health status, BMC Oral Health 24 (2024) 895. https://doi.org/10.1186/s12903-024-04676-x.

[54] A. Costanzo, C. Nowson, L. Orellana, D. Bolhuis, K. Duesing, R. Keast, Effect of dietary fat intake and genetics on fat taste sensitivity: a co-twin randomized controlled trial, Am. J. Clin. Nutr. 107 (2018) 683–694. https://doi.org/10.1093/ajcn/nqy022.

[55] L. Brondel, D. Quilliot, T. Mouillot, N.A. Khan, P. Bastable, V. Boggio, C. Leloup, L. Pénicaud, Taste of fat and obesity: Different hypotheses and our Point of View, Nutrients 14 (2022) 555. https://doi.org/10.3390/nu14030555.

[56] A.K. Patra, Z. Yu, Genomic insights into the distribution of peptidases and proteolytic capacity among Prevotella and Paraprevotella species, Microbiol. Spectr. 10 (2022) e0218521. https://doi.org/10.1128/spectrum.02185-21.

[57] E. Saha, M. Ben Guebila, V. Fanfani, K.H. Shutta, D.L. DeMeo, J. Quackenbush, C.M. Lopes-Ramos, Aging-associated alterations in gene regulatory networks associate with risk, prognosis and response to therapy in lung adenocarcinoma, NPJ Aging 11 (2025) 61. https://doi.org/10.1038/s41514-025-00247-8.

[58] R.N. Dickerson, G.O. Maish 3rd, M.A. Croce, G. Minard, R.O. Brown, Influence of aging on nitrogen accretion during critical illness, JPEN J. Parenter. Enteral Nutr. 39 (2015) 282–290. https://doi.org/10.1177/0148607113506939.

[59] D.M. Pott, J.G. Vallarino, E. Cruz-Rus, L. Willmitzer, J.F. Sánchez-Sevilla, I. Amaya, S. Osorio, Genetic analysis of phenylpropanoids and antioxidant capacity in strawberry fruit reveals mQTL hotspots and candidate genes, Sci. Rep. 10 (2020) 20197. https://doi.org/10.1038/s41598-020-76946-x.

[60] S. Pinhal, D. Ropers, J. Geiselmann, H. de Jong, Acetate metabolism and the inhibition of bacterial growth by acetate, J. Bacteriol. 201 (2019). https://doi.org/10.1128/JB.00147-19.

[61] A.F. Graham, B.M. Lund, The effect of citric acid on growth of proteolytic strains of Clostridium botulinum, J. Appl. Bacteriol. 61 (1986) 39–49. https://doi.org/10.1111/j.1365-2672.1986.tb03756.x.

[62] X.-S. Li, J.-Z. Xue, Y. Qi, I. Muhammad, H. Wang, X.-Y. Li, Y.-J. Luo, D.-M. Zhu, Y.-H. Gao, L.-C. Kong, H.-X. Ma, Citric acid confers broad antibiotic tolerance through alteration of bacterial metabolism and oxidative stress, Int. J. Mol. Sci. 24 (2023). https://doi.org/10.3390/ijms24109089.

[63] N. Takahashi, Oral microbiome metabolism: From "Who are they?" to "What are they doing?," J. Dent. Res. 94 (2015) 1628–1637. https://doi.org/10.1177/0022034515606045.

[64] J. Carlsson, I.R. Hamilton, Differential toxic effects of lactate and acetate on the metabolism of Streptococcus mutans and Streptococcus sanguis, Oral Microbiol. Immunol. 11 (1996) 412–419. https://doi.org/10.1111/j.1399-302x.1996.tb00204.x.

[65] M. Ashburner, C.A. Ball, J.A. Blake, D. Botstein, H. Butler, J.M. Cherry, A.P. Davis, K. Dolinski, S.S. Dwight, J.T. Eppig, M.A. Harris, D.P. Hill, L. Issel-Tarver, A. Kasarskis, S. Lewis, J.C. Matese, J.E. Richardson, M. Ringwald, G.M. Rubin, G. Sherlock, Gene ontology: tool for the unification of biology. The Gene Ontology Consortium, Nat. Genet. 25 (2000) 25–29. https://doi.org/10.1038/75556.

[66] R. Caspi, R. Billington, I.M. Keseler, A. Kothari, M. Krummenacker, P.E. Midford, W.K. Ong, S. Paley, P. Subhraveti, P.D. Karp, The MetaCyc database of metabolic pathways and enzymes - a 2019 update, Nucleic Acids Res. 48 (2020) D445–D453. https://doi.org/10.1093/nar/gkz862.

[67] Z. Li, S.K. Nair, Quorum sensing: how bacteria can coordinate activity and synchronize their response to external signals?, Protein Sci. 21 (2012) 1403–1417. https://doi.org/10.1002/pro.2132.

[68] T. Okuda, E. Kokubu, T. Kawana, A. Saito, K. Okuda, K. Ishihara, Synergy in biofilm formation between Fusobacterium nucleatum and Prevotella species, Anaerobe 18 (2012) 110–116. https://doi.org/10.1016/j.anaerobe.2011.09.003.

[69] Y. Zhang, K.N. Thompson, C. Huttenhower, E.A. Franzosa, Statistical approaches for differential expression analysis in metatranscriptomics, Bioinformatics 37 (2021) i34–i41. https://doi.org/10.1093/bioinformatics/btab327.

[70] C.A. Hempel, N. Wright, J. Harvie, J.S. Hleap, S.J. Adamowicz, D. Steinke, Metagenomics versus total RNA sequencing: most accurate data-processing tools, microbial identification accuracy and perspectives for ecological assessments, Nucleic Acids Res. 50 (2022) 9279–9293. https://doi.org/10.1093/nar/gkac689.

[71] N. Garg, A. Sethupathy, R. Tuwani, R. Nk, S. Dokania, A. Iyer, A. Gupta, S. Agrawal, N. Singh, S. Shukla, K. Kathuria, R. Badhwar, R. Kanji, A. Jain, A. Kaur, R. Nagpal, G. Bagler, FlavorDB: a database of flavor molecules, Nucleic Acids Res. 46 (2018) D1210–D1216. https://doi.org/10.1093/nar/gkx957.

[72] C. Rojas, D. Ballabio, K. Pacheco Sarmiento, E. Pacheco Jaramillo, M. Mendoza, F. García, ChemTastesDB: A curated database of molecular tastants, Food Chem. (Oxf.) 4 (2022) 100090. https://doi.org/10.1016/j.fochms.2022.100090.

[73] M. Mahdizade Ari, K.J. Scholz, F. Cieplik, A. Al-Ahmad, Viable but non-cultivable state in oral microbiota: a critical review of an underexplored microbial survival strategy, Front. Cell. Infect. Microbiol. 15 (2025) 1533768. https://doi.org/10.3389/fcimb.2025.1533768.